

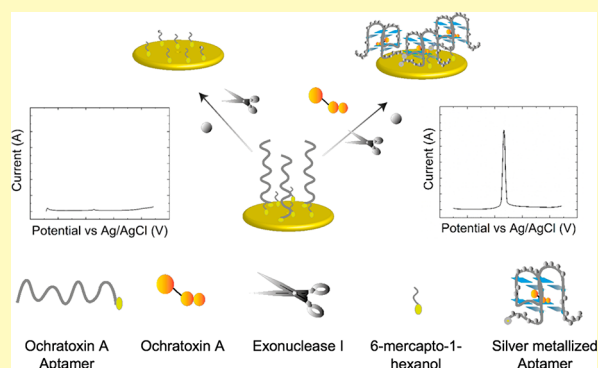
An Exonuclease I-Assisted Silver-Metallized Electrochemical Aptasensor for Ochratoxin A Detection

Akkapol Suea-Ngam,[†] Philip D. Howes,[†] Claire E. Stanley,[‡] and Andrew J. deMello^{*,†}[†]Institute for Chemical and Bioengineering, Department of Chemistry and Applied Biosciences, ETH Zürich, 8093 Zürich, Switzerland[‡]Agroecology and Environment Research Division, Agroscope, 8046 Zürich, Switzerland**S** Supporting Information

ABSTRACT: Ochratoxin A (OTA)—a mycotoxin produced by *Aspergillus* and *Penicillium* fungi—is a carcinogen and common trace contaminant in agricultural and processed food products. As consumption is detrimental to human and animal health, regular product monitoring is vital, and highly sensitive and portable OTA sensors are necessary in many circumstances. Herein, we report an ultrasensitive, electroanalytical aptasensor for precise determination of OTA at trace levels. The sensor leverages a DNA aptamer to capture OTA and silver metallization as a signal enhancer. Exonuclease I is used to digest unbound aptamers, engendering excellent background signal suppression and sensitivity enhancements. Efficient optimization of assay conditions is achieved using central composite design (CCD), allowing rapid evaluation of both

the electrode and square wave voltammetry parameter space. The sensor exhibits excellent analytical performance, with a concentration limit of detection of 0.7 pg mL⁻¹, a limit of quantitation of 2.48 pg mL⁻¹, and a linear dynamic range ($R^2 = 0.968$) of over 6 orders of magnitude (between 1 pg mL⁻¹ and 0.1 μg mL⁻¹). Direct comparison with ultraperformance liquid chromatography (UPLC) indicates excellent analytical performance for standard solutions ($R^2 = 0.995$) and spiked beer samples ($R^2 = 0.993$), with almost quantitative recovery and less than 5% relative standard deviation (RSD).

KEYWORDS: Ochratoxin A, electrochemical detection, square wave voltammetry, DNA metallization, Exonuclease I, central composite design



Ochratoxin A (OTA) is a mycotoxin produced by various types of *Aspergillus* and *Penicillium* fungi. It is classified as a carcinogen to humans (Group 2B) by the International Agency for Research on Cancer.¹ It is commonly found in food products, including wheat, corn, coffee, wine, beer, and nuts because of the difficulty in controlling fungal growth, particularly in soil environments.² The current gold-standard for OTA detection uses HPLC coupled with fluorescence detection,³ but this is operationally complex, costly, and limited for use in well-equipped laboratories. Accordingly, there is a need for efficient, cheap, and rapid analytical tools for application in nonlaboratory and in-the-field environments.⁴

Electrochemical detection is commonly used in toxin analysis⁵ and, due to its instrumental simplicity and high sensitivity, shows great promise for food and environmental control in nonlaboratory or resource-limited settings.^{6,7} Electrochemical detection is frequently facilitated through the use of biorecognition elements such as DNA, enzymes, and antibodies. Aptasensors, which use artificial oligonucleotides (aptamers) as recognition elements in biosensing, have recently been exploited as efficient and inexpensive biorecognition elements.⁸ Indeed, such sensing platforms have found application in food control for detecting toxins from

fungi, bacteria, algae, viruses, drugs, pesticide residues, and heavy metals.⁹

In a typical aptasensor, complementary DNA is used to facilitate binding of reporters, which in turn generate an electrochemical signal.^{10–12} However, such an approach increases both assay complexity and associated costs, and thus it is preferable to use only single-stranded DNA (ssDNA), without a complementary probe. Significantly, aptamers can be directly modified with redox active labels (such as methylene blue and ferrocene), to effect their use as ssDNA electrochemical probes.^{13,14} However, with only one dye molecule per aptamer, at either the 3' or 5' end, signal generation capacity is severely limited. Furthermore, such dye-modified aptamers can only be efficiently conjugated to electrode surfaces at densities of below 10¹³ molecules/cm².¹⁵ Since the extraction of well-defined electrochemical signals requires dye coverages of ~6 × 10¹⁵ molecules cm⁻², both sensitivity and limits of detection are severely compromised.¹⁶ To address this issue, DNA metallization (where electrostatic attraction between negatively

Received: February 1, 2019

Accepted: May 7, 2019

Published: May 7, 2019

charged DNA and positively charged metal ions is used to form metal nanowires subsequent to the application of a reducing agent or electric potential) can be used to realize sensitive biological sensing.¹⁷ For example, Wang and co-workers have used silver metallization on DNA structures to obtain well-defined electrochemical signals,¹⁸ with the basic method subsequently being used in a number of bioanalytical applications.¹⁹ That said, although DNA metallization can provide for large enhancements in electrochemical signal, problems with excessive background currents have limited its application.²⁰ In an effort to address this problem, Wu et al. used exonuclease III, an enzyme that performs a unistrand 3' to 5' end digestion in double-stranded DNA (dsDNA), within a DNA-based electrochemical system to digest unoccupied DNA probes.²¹ This approach successfully reduced background currents, and in turn enhanced both the sensitivity and selectivity of the detection process. Inspired by these advances, we herein report an electrochemical sensor for OTA detection using silver metallization of aptamers on disposable screen-printed gold electrodes (SPGEs), with sensitivity and selectivity enhancements effected by exonuclease I (Exo I). Exo I acts to digest ssDNA in the 3' to 5' direction, and thus removes unoccupied aptamers but cannot act on the G-quadruplex formed upon OTA binding. This significantly reduces nonspecific background metallization. Additionally, both chemical and electrochemical reduction are used to further enhance analytical sensitivity. For assay optimization we employ a central composite design (CCD) approach to explore assay parameter space in a rapid and efficient manner.²² Finally, the resulting sensor platform is used to detect and quantify OTA in commercial beverage samples.

MATERIALS AND METHODS

Materials and Reagents. The OTA aptamer (5'-HS(CH₂)₆ AAA AAA AAA AGAT CGG GTG TGG GTG GCG TAA AGG GAG CAT CGG ACA-3') was purchased from Microsynth (Balgach, Switzerland).²³ Ochratoxin A (OTA), Aflatoxin B1 (AFB1), Aflatoxin B2 (AFB2), AgNO₃, NaBH₄, HEPES, EDTA, Trizma base, NaNO₃, CaCl₂, 6-mercaptop-1-hexanol (MCH), K₃[Fe(CN)₆], K₄[Fe(CN)₆], PBS tablets, NaOH, H₂SO₄, NaCl, and KCl were purchased from Sigma-Aldrich (Buchs, Switzerland) and used as received. All other reagents, including Ochratoxin B (OTB) (AdipoGen AG, Epalinges, Switzerland), TCEP (Alfa Aesar, Karlsruhe, Germany), HCl (Fluka, Buchs, Switzerland), and MgCl₂ (Acros Organics, Geel, Belgium), were analytical reagent grade and used as received. Exo I was purchased from New England Biolabs (Frankfurt am Main, Germany). All aqueous solutions were prepared with DNase and RNase free water (Thermo Fisher Scientific, Reinach, Switzerland). Electrochemical measurements were performed with a PGSTAT204 AutoLab (Metrohm, Zofingen, Switzerland). Screen-printed gold electrodes were purchased from Dropsens (Metrohm, Zofingen, Switzerland). Cyclic voltammetry (CV) data for conductivity characterization were collected at 100 mV s⁻¹ in 10 mM K₃[Fe(CN)₆], 1 M KCl, and 100 mM PBS (pH 7.42) unless otherwise indicated. Electrochemical impedance spectroscopy (EIS) was performed using an Impedance Analyzer SP-300 (Bio-Logic, Seyssinet-Pariset, France) in 0.1 M PBS containing 10 mM K₃[Fe(CN)₆]/K₄[Fe(CN)₆] (1:1), with 1 M KCl as the supporting electrolyte. Impedance spectra were recorded at frequencies between 10⁻² and 10⁵ Hz. The applied potential was 0.2 V with a sinusoidal potential of 5 mV amplitude.

Electrochemical Detection. SPGEs were electrochemically cleaned using a series of oxidation and reduction cycles in 0.5 M NaOH, 0.5 M H₂SO₄, 0.01 M KCl with 0.1 M H₂SO₄, and 0.05 M H₂SO₄, using cyclic voltammetry (100 mV s⁻¹, from -1 to 1 V) prior to modification with the thiolated OTA aptamer. For sample analysis,

different concentrations of the thiolated OTA aptamer were pretreated with 10 mM TCEP in buffer (10 mM Tris-HCl, 1 mM EDTA, 0.1 M NaCl, pH 7.4) for 30 min to reduce thiol–thiol bonds. Next, 10 μL of the reduced aptamer solution was dropped onto the electrochemically cleaned electrode surface, and kept under high humidity in the dark and at room temperature for 12 h. Subsequently, the modified surface was rinsed with buffer solution and then passivated with MCH in Tris-HCl buffer (pH 8.3) for 30 min. After washing, the electrode was dried using nitrogen gas, and again stored in the dark under nitrogen.

For electrochemical detection, modified electrodes were immersed for 10 min in the sample, as prepared in binding buffer (10 mM Tris, pH 8.5, 120 mM NaCl, 5 mM KCl, 10 mM MgCl₂, and 20 mM CaCl₂). Next, 50 μL of Exo I enzyme solution (100–500 U mL⁻¹) was applied to the electrode, at room temperature, to digest excess aptamer. The washed electrode was then immersed in 100 μM AgNO₃ in 20 mM HEPES and 100 mM NaNO₃ (pH 7.4) for 1 h and subsequently washed with water. Next, the modified electrode was dipped into a freshly prepared 10 mM of NaBH₄ (in 20 mM HEPES buffer) for 10 min, washed with water and placed in an electrolyte (0.1 M NaCl and 0.1 M NaNO₃) for the electrochemical measurement. Electrochemical deposition was achieved with a -0.5 V applied potential prior to square wave voltammetry from -0.3 to 0.5 V versus Ag/AgCl.

System Optimization. Central composite design (CCD) was used to optimize key experimental variables including aptamer concentration, enzyme concentration, and incubation time. All studied parameters were considered to be independent. The ranges and levels of the chosen variables are reported in Table 1. Three

Table 1. Experimental Range and Level of the Respective Independent Variables for Electrode Optimization

variables (unit)	actual			coded level		
	low	middle	high	low	middle	high
Aptamer concentration (μM)	0.5	1	1.5	-1	0	1
Enzyme concentration (U mL ⁻¹)	200	300	400	-1	0	1
Incubation time (minutes)	30	60	90	-1	0	1

factors with a total of 20 experimental runs were suggested by CCD, as displayed in Table 2.²⁴ Response surface modeling, statistical analysis, and optimization were conducted using the matrix shown in Table S1 and eqs S1 and S2. Paired *t* tests and coefficients of determination (*R*²) were used in the analysis of output data. Currents were normalized using the percentage difference between the analyte peak and the background as shown in eq 1.

$$\text{Normalized current(\%)} = \frac{|I_{\text{peak}} - I_{\text{background}}|}{I_{\text{peak}}} \times 100 \quad (1)$$

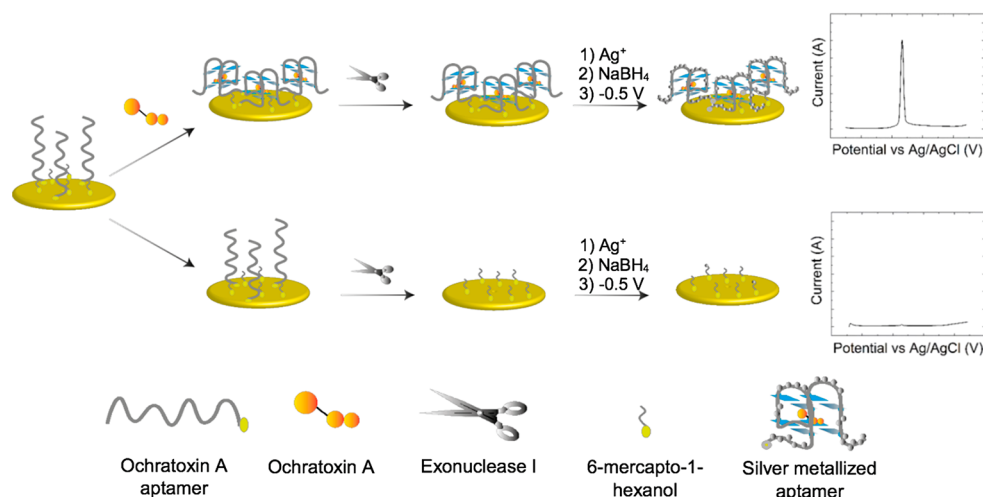
Here, *I*_{peak} is the current obtained in the presence of the analyte, and *I*_{background} is the current obtained in absence of the analyte. Response data from experiments were expressed by polynomial regression to generate the model shown in eq 2.

$$y = \text{intercept} + \sum_{i=1}^n b_i X_i + \sum_{i=1}^n b_{ii} X_i^2 + \sum_{i=1}^{n-1} \sum_{j=i+1}^n b_{ij} X_i X_j \quad (2)$$

Here *y* represents the predicted responses, *b*_{*i*} is the linear coefficient, *b*_{*ii*} is the quadratic coefficient, *b*_{*ij*} is the interaction coefficient, while *X*_{*i*} and *X*_{*j*} represent variables. Optimum values of variables were predicted by response surface analysis of the combined variables. The constraints in this study were applied to predict the optimum variable conditions that would yield the highest normalized current by inserting the desired conditions into the design shown in Table 2. The efficiency of the model was evaluated by performing the suggested experiments and comparing the output with the predicted

Table 2. Central Composite Design for Electrode Optimization Using Aptamer Concentration, Enzyme Concentration, Incubation Time, and Normalized Peak Current Response Data

run	aptamer (μM)	enzyme (U mL^{-1})	incubation time (minutes)	%difference of peak and background	
				experiment	predicted
1	1.5 (1)	400 (1)	90 (1)	84.45	81.54
2	1.5 (1)	401 (1)	30 (-1)	79.37	82.25
3	1.5 (1)	200 (-1)	90 (1)	76.55	78.03
4	1.5 (1)	200 (-1)	30 (-1)	62.57	60.99
5	0.5 (-1)	400 (1)	90 (1)	87.73	87.81
6	0.5 (-1)	401 (1)	30 (-1)	77.82	74.83
7	0.5 (-1)	200 (-1)	90 (1)	90.92	86.54
8	0.5 (-1)	200 (-1)	30 (-1)	54.40	55.81
9	1.84 (1.68)	300 (0)	60 (0)	83.46	82.82
10	0.16 (-1.68)	300 (0)	60 (0)	80.96	83.73
11	1 (1)	468 (1.68)	60 (0)	81.84	82.87
12	1 (1)	132 (-1.68)	60 (0)	62.84	63.94
13	1 (1)	300 (0)	110.4 (1.68)	81.01	83.69
14	1 (1)	300 (0)	9.6 (-1.68)	59.02	58.47
15	1 (1)	300 (0)	60 (0)	75.08	75.03
16	1 (1)	300 (0)	60 (0)	74.91	75.03
17	1 (1)	300 (0)	60 (0)	74.64	75.03
18	1 (1)	300 (0)	60 (0)	74.66	75.03
19	1 (1)	300 (0)	60 (0)	75.96	75.03
20	1 (1)	300 (0)	60 (0)	75.33	75.03

Scheme 1. Schematic Illustration of the Silver Metallization Assay for OTA Detection Using Enzyme-Assisted Background Current Suppression

results. The coefficient of determination (R^2) and t -test (paired) were used to determine model robustness. The numerical optimization of the response was predicted based on a second order polynomial model.

For square wave voltammetry parameters, CCD was used to determine the step potential, amplitude, and frequency using a similar protocol as described for electrode optimizations, as shown in Table S3. In addition, peak potential and peak full-width-half-maximum (fwhm) were used to identify optimum values for square wave voltammetry.

Real Sample Analysis. Ultrapformance liquid chromatography (UPLC) was used to compare both standard OTA solutions and spiked-beer samples, obtained from a local store, using conditions as reported by Wei et al.²⁵ Beer samples were degassed with argon gas before being directly applied to either the aptasensor electrode or UPLC analysis. Testing was performed by spiking OTA into beer at concentrations of 1, 10, and 100 ng mL^{-1} .

RESULTS AND DISCUSSION

The electrochemical aptasensor system described herein solves problems associated with both matrix interference in solution-based reactions and high background signals from DNA metallization. The assay procedure is illustrated in Scheme 1. OTA from the sample binds to the aptamer on the electrode surface, forming a G-quadruplex.²³ Exo I is introduced to digest unoccupied aptamers, leaving only G-quadruplexes that cannot be digested. Next, a Ag^+ solution is applied (activation step), followed by a reducing agent (NaBH_4) to form silver metallized aptamers (reduction step). Further reduction is achieved by applying a potential lower (more negative) than the reduction potential of Ag^+ , to form additional Ag .¹⁷ Finally, square wave voltammetry is used to detect the silver-metallized aptamer.

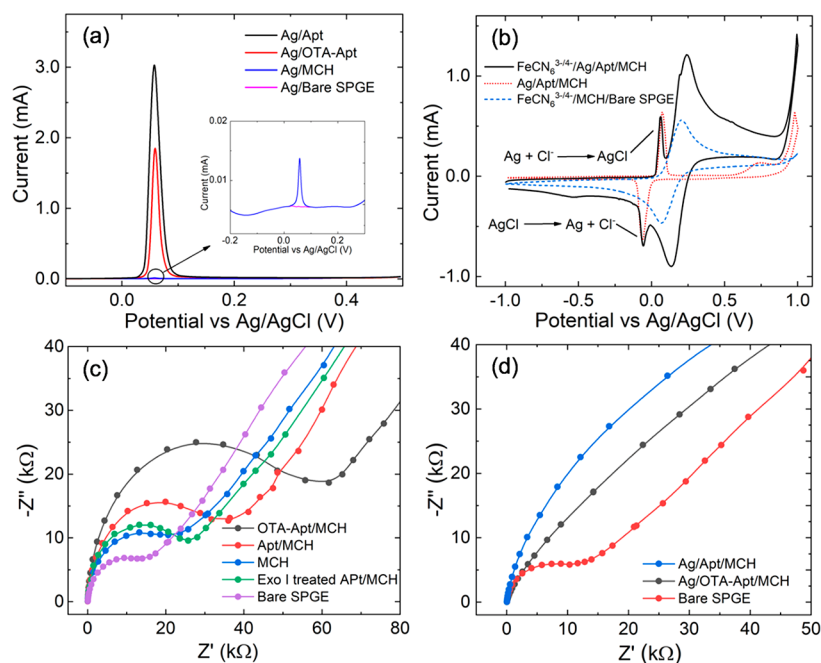


Figure 1. MCH modified (MCH), aptamer modified (Apt), ochratoxin A-aptamer modified (OTA-Apt), and screen-printed gold electrodes (SPGE) were compared using (a) square wave voltammetry, (b) cyclic voltammetry, and (c,d) electrochemical impedance spectroscopy. Square wave voltammograms of silver-metallized electrodes were carried out using a potential step of 0.01 V, an amplitude of 0.06 V, and a frequency of 200 Hz. For cyclic voltammograms and Nyquist plots, 10 mM $[\text{Fe}(\text{CN})_6]^{3-/4-}$ in 0.1 M PBS were used as the working solution and 0.1 M PBS was used as the background electrolyte. The reversible cyclic voltammograms were carried out using a scan rate of 100 mV s^{-1} , while Nyquist plots were obtained by applying a 5 mV sine wave potential within a frequency range of 10^{-2} to 10^5 Hz.

Characterization of Modified Electrodes. Silver-metalized electrodes were investigated using a range of electrochemical methods. Figure 1a shows square wave voltammograms of the bare SPGE, MCH modified (MCH), aptamer and MCH modified (Apt/MCH) and OTA-aptamer and MCH modified (OTA-Apt/MCH) electrodes, illustrating well-defined peaks from the Apt/MCH and OTA-Apt/MCH electrodes. Data were in good agreement with previous reports,^{26,27} and can be explained by consideration of electrostatic attraction between the negatively charged aptamers and positively charged Ag^+ . Figure 1b shows reversible cyclic voltammograms of the silver metallized aptamers, suggesting chemical reduction–oxidation. In the presence of 10 mM $[\text{Fe}(\text{CN})_6]^{3-/4-}$, the cathodic and anodic peaks of the metallized aptamer showed greater peak currents than the unmodified electrode. The increase in the voltammetric peaks obtained with metallized DNA on the working electrode surface could be indicative of an increased electroactive surface area due to solid silver deposition on the DNA.²⁸ Significantly, silver chloride redox peaks were observed in cyclic voltammograms of $[\text{Fe}(\text{CN})_6]^{3-/4-}$ in the presence of the metallized aptamer, suggesting both an increased active electrode area and conductivity.

Electrochemical impedance spectroscopy (EIS) was then used to evaluate the success of electrode modification with the aptamer. EIS is an effective method for evaluating the interfacial electron transfer efficiency at different stages of biosensor preparation, since each step can be evaluated by monitoring the change in electron transfer resistance (R_{ct}), as read from the EIS plot.²⁹ As shown in Figure 1c, the R_{ct} of the bare SPGE was the lowest, which implies that the electroactive ions of $[\text{Fe}(\text{CN})_6]^{3-/4-}$ are rapidly transported to the electrode interface. After MCH modification of the electrode the R_{ct}

value increased, which is in line with an expected decrease in transport kinetics due to impairment by the MCH. Self-assembly of the thiolated aptamer onto the electrode surface led to a significant increase in R_{ct} , since oligonucleotides exhibit low electroactivity. The R_{ct} increased significantly upon further addition of OTA, due to the steric effect of the OTA-aptamer G-quadruplex structure hindering electro-active species from reaching the electrode surface. When ExoI was used to digest the unoccupied aptamers from an aptamer-modified electrode (Apt/MCH, no OTA), the R_{ct} value was only marginally different from the MCH-modified electrode, indicating full DNA digestion, leaving only MCH on the electrode surface. The dome-shaped portions of the plots in Figure 1c indicate a kinetically controlled domain, and suggest impairment of electron transport to the electrode surface. This characteristic disappeared after silver metallization of Apt/MCH and OTA-Apt/MCH electrodes, as shown in Figure 1d. Yet, silver metallization of the MCH electrode exhibited only a slight difference after metallization. In addition, coulometric analysis was carried out using a 0.2 V applied potential for a duration of 60 s, comparing the bare, aptamer-modified and silver-metallized aptamer-modified electrodes (Figure S1). Charge was calculated from the area under the $i-t$ curve, and the amount of silver deposited was calculated to be 38.8 ng on the aptamer-modified electrode. This result confirmed that silver metallization of the DNA was successful. Together, these results indicate rapid kinetics in the silver-metallized electrodes, due to the deposition of solid silver on the DNA. In summary, the EIS data confirm that aptamer modification, aptamer binding, and aptamer metallization on the SPGE were successful.

Optimization. Aptamer Silver Metallization. DNA metallization usually proceeds via three steps: activation,

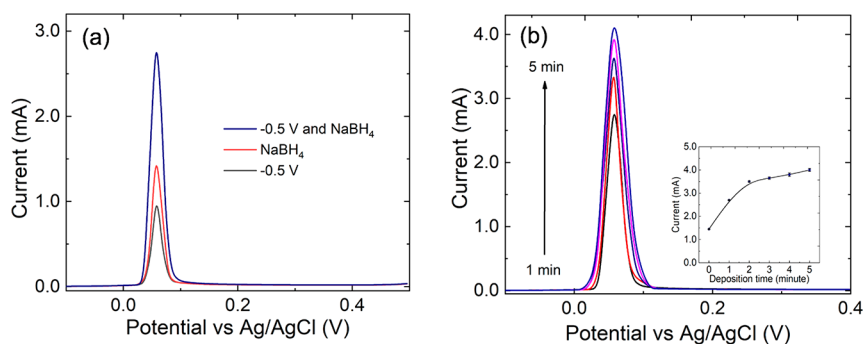


Figure 2. (a) Square wave voltammograms of silver metallization comparing chemical, electrochemical, and combined reductions. (b) Deposition time of Ag on the aptamer-modified SPGE. An applied potential of -0.5 V, a potential step of 0.01 V, an amplitude of 0.06 V, and a frequency of 200 Hz were used.

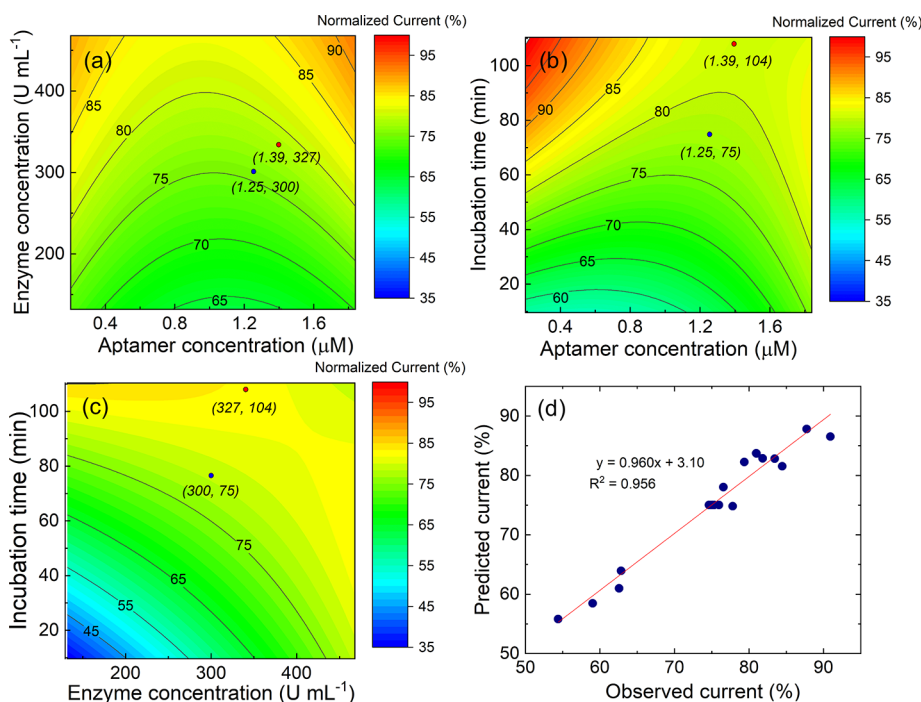


Figure 3. Surface contour plots of the percentage difference between peak current and background as a function of (a) concentration of aptamer and enzyme, (b) concentration of aptamer and incubation time, and (c) enzyme concentration and incubation time. The red points indicate the theoretical optimum values, and the blue points indicate the practical optimum values. (d) Plot of the predicted values as obtained from regression (eq 3) against experimental values.

reduction, and growth. For the reduction step, either chemical or electrochemical reduction is utilized. The combination of both reduction methods has not been reported previously. Herein, we observed that metallization using only a reducing agent provided a higher electrochemical signal compared to voltage-induced metallization, as illustrated in Figure 2a. Furthermore, we observed that a combination of both methods increased the electrochemical signal by a factor of 2. Specifically, an applied potential of -0.5 V (vs Ag/AgCl) was chosen. This is lower than the reduction potential of AgCl to Ag as indicated in the cyclic voltammogram (Figure 1b). An electrochemical reduction time of 3 min was observed to provide the highest electrochemical signal, allowing for full growth of silver on the aptamer (Figure 2b).

Central Composite Design. Having established the working principle of the OTA aptasensor electrode, we then set out to establish which experimental parameters yield optimal signal strength. We used central composite design as the analytical

optimization model. CCD not only minimizes the number of experimental trials, but also provides linear, quadratic, and interaction information, which is inaccessible through a one-factor-at-the-time approach. Table 1 and Figure S2 show the independent variables tested, as well as their actual and associated coded values, the latter being used to avoid experimental bias. CCD analysis was performed as described in the Methods section, using the model shown in Table 2. This resulted in the following polynomial regression

$$\begin{aligned}
 y = & 75.03 - 0.27(\text{Aptamer}) + 5.63(\text{Enzyme}) \\
 & + 7.51(\text{Time}) + 2.92(\text{Aptamer})^2 - 0.58(\text{Enzyme})^2 \\
 & - 1.40(\text{Time})^2 + 0.56(\text{Aptamer} \times \text{Enzyme}) \\
 & - 3.42(\text{Aptamer} \times \text{Time}) - 4.44(\text{Enzyme} \times \text{Time})
 \end{aligned}
 \quad (3)$$

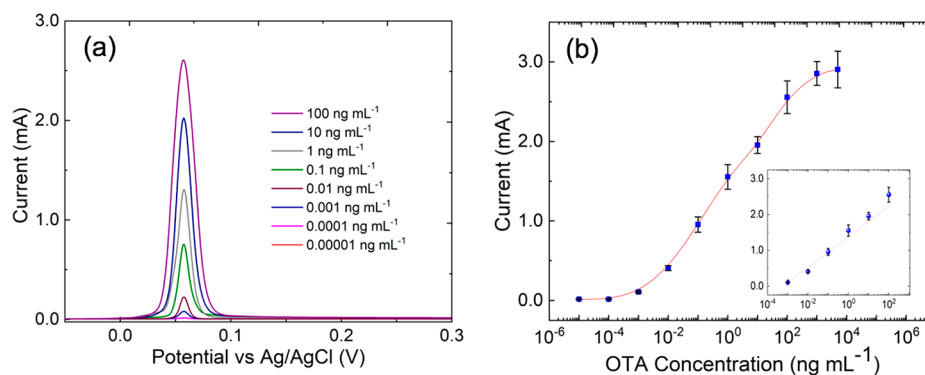


Figure 4. (a) Square wave voltammograms of a series of OTA concentrations from 10^{-5} to 10^2 using the CCD-optimized conditions: an aptamer concentration of $1.25 \mu\text{M}$, an enzyme concentration of 375 U mL^{-1} , an incubation time of 75 min, a step potential of 0.01 V, an amplitude of 0.06 V, and a frequency of 200 Hz. (b) Calibration curve of anodic current ($N = 5$) obtained from (a), versus OTA concentration showing a linear range from 10^{-3} to 10^2 ng mL^{-1} , as shown in the inset.

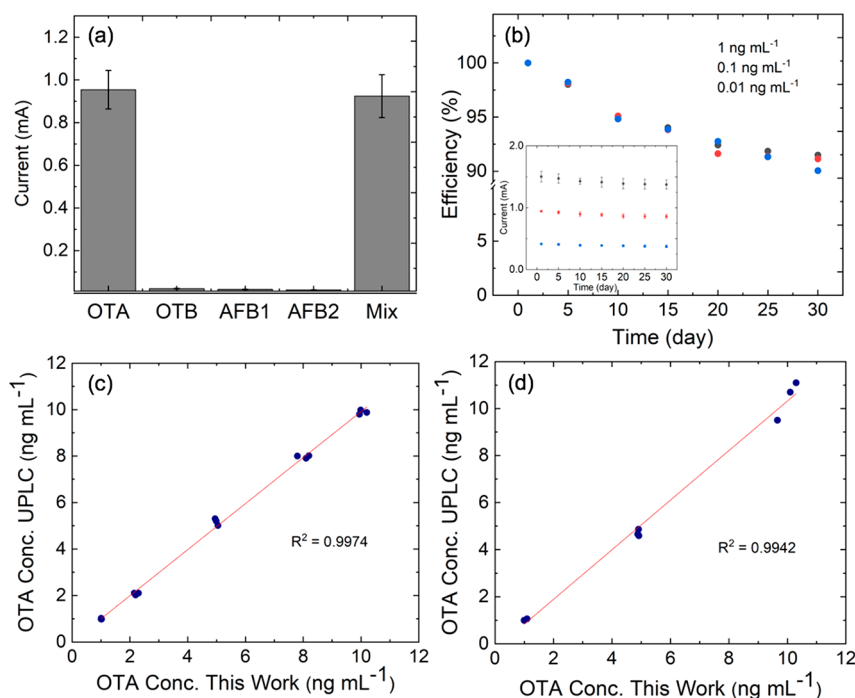


Figure 5. (a) Electrochemical signal from the silver-metallized aptasensor in the presence of potential interferents, with OTB and AFB2 concentrations of 1.0 ng mL^{-1} , an OTA concentration of 0.1 ng mL^{-1} , and their mixture ($N = 3$). (b) Stability of the electrochemical aptasensor for detecting OTA (0.01 , 0.1 , and 1 ng mL^{-1}) over 30 days ($N = 3$). Comparison of OTA concentrations between the electrochemical aptasensor and UPLC carried out from the (c) standard solutions and (d) spiked beer samples.

which provides the percentage difference between the electrochemical signal and the background current. The predicted values obtained from eq 3 were compared with experimental data (shown in Table 2). Paired t -tests showed that the experimental and predicted data sets ($n = 20$) are not significantly different, as the t -value (0.002) is smaller than t -critical (2.09). Furthermore, both experimental and predicted data were compared and shown to exhibit excellent correspondence ($R^2 = 0.956$) (Figure 3d).

Equation 3 yields theoretical optimal values of $1.39 \mu\text{M}$, 327 U mL^{-1} , and 104 min for aptamer concentration, enzyme concentration, and incubation time, respectively. These values gave a predicted a response of 80% normalized current for 1 ng mL^{-1} of OTA. To optimize the practical value of the assay, we sought to further reduce the assay time and reagent consumption (enzyme and aptamer). This was done by

consulting the CCD model data (Figure 3a–c) and deriving minimized parameter values that would still yield a sufficient normalized current. Setting a threshold of 78% predicted normalized current (i.e., a 2% reduction), practical optimal values of $1.25 \mu\text{M}$, 300 U mL^{-1} , and 75 min were obtained, for aptamer concentration, enzyme concentration, and incubation time, respectively. Thus, for a minor reduction in signal, significant reductions in assay time and reagent consumption were achieved.

Next, we attempted to optimize the square wave voltammetry variables of amplitude, voltage step, and frequency. These control peak current, as shown in eq 4.

$$i_p = \frac{nFAD^{1/2}C^*}{\pi^{1/2}t_p^{1/2}}\varphi_p(\Delta E_s, E_p) \quad (4)$$

Table 3. Determination of OTA Concentration in Spiked Beer Samples Comparing the Electrochemical Aptasensor with UPLC

sample	spiked OTA (ng mL ⁻¹)	detected (ng mL ⁻¹)		recovery (%)		%RSD		<i>t</i> -value
		this study	UPLC	this study	UPLC	this study	UPLC	
Beer 1	1	1.00 ± 0.01	1.00 ± 0.02	100.4	99.69	1.04	2.63	0.28
	5	4.91 ± 0.03	4.86 ± 0.05	98.13	97.29	1.36	1.98	0.28
	10	9.66 ± 0.18	9.50 ± 0.32	96.57	94.97	1.45	1.01	0.08
Beer 2	1	1.00 ± 0.02	0.99 ± 0.04	100.4	99.17	0.49	0.46	0.06
	5	4.88 ± 0.04	4.66 ± 0.10	97.54	93.14	0.47	1.61	0.01
	10	10.3 ± 0.21	11.1 ± 0.31	103.4	110.7	1.58	0.55	0.01
Beer 3	1	1.10 ± 0.01	1.06 ± 0.05	109.7	105.8	0.55	1.41	0.04
	5	4.92 ± 0.05	4.59 ± 0.12	98.40	91.81	0.61	1.41	0.01
	10	10.1 ± 0.25	10.7 ± 0.35	100.9	107.5	1.97	0.70	0.01

Here, i_p is the measured current during each pulse (A), n is the number of electrons transferred, F is the Faraday constant ($C\ mol^{-1}$), A is the area of the electrode (cm^2), D is the reactant diffusion constant ($cm^2\ s^{-1}$), C^* is the bulk concentration of the reactant (M), t_p is the pulse width (half of the staircase period) (s), and φ_p is the dimensionless current function which depends on step height (ΔE_s) and square wave amplitude (E_p).^{30,31}

After applying CCD for square wave voltammetry optimization, the model suggested using the maximum value for all variables (as shown in Figure S3 and Figure S4). For further analysis, we took into consideration the peak height, peak position, and peak full-width-half-maximum (fwhm) as indicators of the optimum variable combination, where the peak height should be as high as possible, peak position of silver oxidation versus Ag/AgCl should be at 0 V, and the fwhm should be 90.5 mV (corresponding to one electron involved in the redox reaction).³² These conditions are indicated as bound regions in (Figure S5). From this, the practical optimum values obtained were an applied step potential of 0.01 V, an amplitude of 0.06 V, and a frequency of 200 Hz.

Analytical Performance. *Dynamic Range, Limit of Detection, and Limit of Quantitation.* After obtaining optimum values for each variable, a calibration curve was constructed using an OTA concentration series between 10^{-5} and $10^4\ ng\ mL^{-1}$. Using the optimized parameters, square wave voltammograms at each concentration were obtained, as shown in Figure 4a. The obtained electrochemical peak values ($N = 5$) were plotted against concentration, shown in the calibration curve in Figure 4b, yielding a linear range between 10^{-3} and $10^2\ ng\ mL^{-1}$ (Figure 4b inset). The limit of detection (LOD) and limit of quantitation (LOQ) were calculated using 3 and 10 times the background standard deviation, respectively, and determined from fits to the calibration curve. An LOD of $0.7\ pg\ mL^{-1}$ and an LOQ of $2.48\ pg\ mL^{-1}$ were obtained.

The analytical performance of the electrochemical aptasensor was compared with published studies on the electrochemical detection of OTA, as shown in Table S4. Significantly, the current approach provides a lower LOD and wider working range compared to other silver metallization assays.^{33–43} The LOD of our system is marginally higher than the platforms presented in refs 44,45; however, it is important to note that the linear range in the current system is much wider and the method far simpler to implement due to the use of disposable SPGEs.

Selectivity and Stability. The selectivity of our electrochemical aptasensor was assessed by examining its response to potential (and common) interferents, including ochratoxin B (OTB), aflatoxin B1 (AFB1), and aflatoxin B2 (AFB2). In the current experiments, the concentration of each interferent ($1.0\ ng\ mL^{-1}$) was made 1 order of magnitude higher than that of OTA ($0.1\ ng\ mL^{-1}$). The results of the selectivity assessment are shown in Figure 5a. In contrast to the significant square wave voltammetry signal of OTA and a mixed solution containing OTA, a negligible response was observed on addition of all interferents. This indicated excellent selectivity of the electrochemical aptasensor for OTA over the OTB, AFB1, and AFB2, which was attributable to the high selectivity of the aptamer probe sequence.

Stability over time and reproducibility are key factors in the practical application of sensing systems. To test storage stability, aptasensors were kept at $4\ ^\circ C$ under nitrogen for up to 30 days, with square wave voltammetry then used to study the electrochemical response for 0.01 , 0.1 , and $1\ ng\ mL^{-1}$ OTA using the optimum conditions (Figure 5b). It should be noted that electrodes were not reused, due to the silver reduction occurring directly on the aptamer structure. Data indicate a minimal change in response to a series of OTA concentrations in comparison to a freshly prepared electrode. A *t*-test comparison showed no significant difference between the fresh and stored electrodes (*t*-values for the three concentrations were 0.09, 0.02, and 0.001 for 0.01 , 0.1 , and $1\ ng\ mL^{-1}$, respectively, where *t*-critical = 1.94). However, the average current of the stored electrode did exhibit a 10% reduction in electrochemical signal (shown in the inset of Figure 5b), which is likely a result of partial decomposition or deconjugation of the aptamer on the electrode surface.

Real Sample Analysis. The results using model samples indicate that the electrochemical aptasensor exhibits excellent biosensing performance, including high sensitivity, high selectivity, high stability, and good reproducibility. To further validate the sensor, it was compared to the gold standard UPLC method, using OTA concentrations between 1 and $10\ ng\ mL^{-1}$. Data presented in Figure 5c, show excellent agreement between the detection methods ($R^2 = 0.995$). Finally, to verify the practical applicability of the electrochemical aptasensor, sensing was performed using a real sample matrix, with beer chosen as an exemplar system. Different OTA concentrations (1 , 5 , and $10\ ng\ mL^{-1}$) were spiked into the degassed beer samples, and the presence of OTA detected and quantified using the aptasensor calibration curve shown in Figure 4b. As shown in Table 3, recovery ranged from 96.6% to 109.7%, with an RSD of less than 5%.

The obtained results were compared to UPLC, confirming excellent correspondence ($R^2 = 0.994$, as shown in Figure 5d), and demonstrating the potential for use with real samples.

CONCLUSIONS

We have presented a novel electroanalytical method to detect OTA using an enzyme-assisted silver-metallized aptasensor. The aptamers, which were readily conjugated to disposable SPGEs, exhibited excellent specificity for the target analyte. Degradation of unoccupied aptamers after addition of the test sample was performed by the enzyme Exo I, which significantly reduced the background signal and increased sensitivity. Addition of AgCl followed by a double reduction method metallized the target-bound aptamers, yielding a significant signal enhancement in square wave voltammetry-based measurements. Electrode preparation variables and square wave voltammetry parameters were optimized using central composite design, which allowed efficient and rapid assay optimization. The resultant electrochemical aptasensor exhibited an LOD of 0.7 pg mL^{-1} , an LOQ of 2.48 pg mL^{-1} , and a linear range between 0.001 and 100 ng mL^{-1} (6 orders of magnitude) against standard OTA solutions. The electrochemical aptasensor was compared to gold-standard UPLC analysis, confirming excellent agreement when using both standard and beer-spiked OTA samples. It should be noted that use of an enzyme in such a sensor could pose potential complications for in-the-field application. However, recent advances in the preparation of freeze-dried enzymes on paper-based diagnostic strips,^{46,47} which are stable when stored and reactivated when sample is added, suggest that electrodes could be made using a similar approach. Overall, the developed aptasensor allows the detection of OTA with high sensitivity, selectivity, accuracy, precision, and robustness in real samples.

ASSOCIATED CONTENT

Supporting Information

The Supporting Information is available free of charge on the ACS Publications website at DOI: 10.1021/acssensors.9b00237.

Coulometric analysis; Central composite design operation, testing, and optimization; Electrochemical optimization; Analytical performance comparison (PDF)

AUTHOR INFORMATION

Corresponding Author

*E-mail: andrew.demello@chem.ethz.ch.

ORCID

Philip D. Howes: 0000-0002-1862-8395

Andrew J. deMello: 0000-0003-1943-1356

Notes

The authors declare no competing financial interest.

ACKNOWLEDGMENTS

A.S.N would like to acknowledge a Swiss Government Excellence Scholarship for partial support of his PhD studies. The authors thank Professor Kanet Wongravee, Ms. Mamiko Ninomiya, and Ms. Tain Liu for consulting of CCD, and assistance with UPLC and EIS measurements, respectively. C.E.S acknowledges support from the Swiss National Science Foundation in the form of an Ambizione Career Grant (PZ00P2_168005).

REFERENCES

- (1) International Agency for Research on Cancer, Some naturally occurring substances: food items and constituents, heterocyclic aromatic amines and mycotoxins; *IARC Monographs on the Evaluation of Carcinogenic Risks to Humans*; 1993, Vol 56.
- (2) Alexander, J.; Atrup, H.; Bard, D.; Benford, D.; Carere, A.; Costa, L. G.; Cravedi, J. P.; Di Domenico, A.; Fanelli, R.; Fink-Gremmels, J.; Gilbert, J.; Grandjean, P.; Johansson, N.; Oskarsson, A.; Ruprich, J.; Schlatter, J.; Schoeters, G.; Schrenk, D.; van Leeuwen, R.; Verger, P.; Sci Panel, M. Opinion of the scientific panel on contaminants in the food chain on a request from the commission related to ochratoxin A in food. *EFSA J.* 2006, 4, 1–56.
- (3) Cantafora, A.; Grossi, M.; Miraglia, M.; Benelli, L. Determination of ochratoxin A in coffee beans using reversed-phase high performance liquid chromatography. *Riv. Soc. Ital. Sci. Aliment* 1983, 12, 103–108.
- (4) Meulenbergh, E. P. Immunochemical methods for ochratoxin A detection: a review. *Toxins* 2012, 4, 244–266.
- (5) Reverté, L.; Prieto-Simón, B.; Campàs, M. New advances in electrochemical biosensors for the detection of toxins: Nanomaterials, magnetic beads and microfluidics systems. *Anal. Chim. Acta* 2016, 908, 8–21.
- (6) Rackus, D. G.; Shamsi, M. H.; Wheeler, A. R. Electrochemistry, biosensors and microfluidics: a convergence of fields. *Chem. Soc. Rev.* 2015, 44, 5320–5340.
- (7) Nemiroski, A.; Christodouleas, D. C.; Hennek, J. W.; Kumar, A. A.; Maxwell, E. J.; Fernández-Abedul, M. T.; Whitesides, G. M. Universal mobile electrochemical detector designed for use in resource-limited applications. *Proc. Natl. Acad. Sci. U. S. A.* 2014, 111, 11984–11989.
- (8) Song, S.; Wang, L.; Li, J.; Fan, C.; Zhao, J. Aptamer-based biosensors. *TrAC, Trends Anal. Chem.* 2008, 27, 108–117.
- (9) Duan, N.; Wu, S.; Dai, S.; Gu, H.; Hao, L.; Ye, H.; Wang, Z. Advances in aptasensors for the detection of food contaminants. *Analyst* 2016, 141, 3942–3961.
- (10) Miao, P.; Han, K.; Wang, B.; Luo, G.; Wang, P.; Chen, M.; Tang, Y. Electrochemical detection of aqueous Ag⁺ based on Ag⁺-assisted ligation reaction. *Sci. Rep.* 2015, 5, 1–5.
- (11) Si, Y.; Sun, Z.; Zhang, N.; Qi, W.; Li, S.; Chen, L.; Wang, H. Ultrasensitive electroanalysis of low-level free microRNAs in blood by maximum signal amplification of catalytic silver deposition using alkaline phosphatase-incorporated gold nanoclusters. *Anal. Chem.* 2014, 86, 10406–10414.
- (12) Hsieh, K.; Patterson, A. S.; Ferguson, B. S.; Plaxco, K. W.; Soh, H. T. Rapid, sensitive, and quantitative detection of pathogenic DNA at the point of care through microfluidic electrochemical quantitative loop-mediated isothermal amplification. *Angew. Chem.* 2012, 124, 4980–4984.
- (13) White, R. J.; Plaxco, K. W. Exploiting binding-induced changes in probe flexibility for the optimization of electrochemical biosensors. *Anal. Chem.* 2010, 82, 73–76.
- (14) Li, H.; Dauphin-Ducharme, P.; Ortega, G.; Plaxco, K. W. Calibration-free electrochemical biosensors supporting accurate molecular measurements directly in undiluted whole blood. *J. Am. Chem. Soc.* 2017, 139, 11207–11213.
- (15) Steel, A. B.; Herne, T. M.; Tarlov, M. J. Electrochemical quantitation of DNA immobilized on gold. *Anal. Chem.* 1998, 70, 4670–4677.
- (16) Wang, J.; Wang, F.; Dong, S. Methylene blue as an indicator for sensitive electrochemical detection of adenosine based on aptamer switch. *J. Electro. Chem.* 2009, 626, 1–5.
- (17) Chen, Z.; Liu, C.; Cao, F.; Ren, J.; Qu, X. DNA metallization: principles, methods, structures, and applications. *Chem. Soc. Rev.* 2018, 47, 4017–4072.
- (18) Wang, J.; Xu, D.; Polsky, R. Magnetically-induced solid-state electrochemical detection of DNA hybridization. *J. Am. Chem. Soc.* 2002, 124, 4208–4209.
- (19) Hwang, S.; Kim, E.; Kwak, J. Electrochemical detection of DNA hybridization using biometallization. *Anal. Chem.* 2005, 77, 579–584.

- (20) Wang, J.; Rincón, O.; Polsky, R.; Dominguez, E. Electrochemical detection of DNA hybridization based on DNA-templated assembly of silver cluster. *Electrochem. Commun.* **2003**, *5*, 83–86.
- (21) Wu, L.; Wang, J.; Ren, J.; Qu, X. Ultrasensitive telomerase activity detection in circulating tumor cells based on DNA metallization and sharp solid-state electrochemical techniques. *Adv. Funct. Mater.* **2014**, *24*, 2727–2733.
- (22) Suea-Ngam, A.; Rattanasart, P.; Wongravee, K.; Chailapakul, O.; Srisa-Art, M. Droplet-based glucosamine sensor using gold nanoparticles and polyaniline-modified electrode. *Talanta* **2016**, *158*, 134–141.
- (23) Lv, L.; Li, D.; Liu, R.; Cui, C.; Guo, Z. Label-free aptasensor for ochratoxin A detection using SYBR Gold as a probe. *Sens. Actuators, B* **2017**, *246*, 647–652.
- (24) Talib, N. A. A.; Salam, F.; Yusof, N. A.; Ahmad, S. A. A.; Sulaiman, Y. Optimization of peak current of poly (3, 4-ethylenedioxythiophene)/multi-walled carbon nanotube using response surface methodology/central composite design. *RSC Adv.* **2017**, *7*, 11101–11110.
- (25) Wei, D.; Wu, X.; Xu, J.; Dong, F.; Liu, X.; Zheng, Y.; Ji, M. Determination of ochratoxin A contamination in grapes, processed grape products and animal-derived products using ultra-performance liquid chromatography-tandem mass spectroscopy system. *Sci. Rep.* **2018**, *8*, 1–8.
- (26) Kondo, J.; Tada, Y.; Dairaku, T.; Hattori, Y.; Saneyoshi, H.; Ono, A.; Tanaka, Y. A metallo-DNA nanowire with uninterrupted one-dimensional silver array. *Nat. Chem.* **2017**, *9*, 956–960.
- (27) Chen, X.; Karpenko, A.; Lopez-Acevedo, O. Silver-mediated double helix: structural parameters for a robust DNA building block. *ACS Omega* **2017**, *2*, 7343–7348.
- (28) Suea-Ngam, A.; Rattanasart, P.; Chailapakul, O.; Srisa-Art, M. Electrochemical droplet-based microfluidics using chip-based carbon paste electrodes for high-throughput analysis in pharmaceutical applications. *Anal. Chim. Acta* **2015**, *883*, 45–54.
- (29) Retter, U.; Lohse, H., *Electrochemical impedance spectroscopy*. In *Electroanalytical Methods*; Springer: 2010; pp 159–177.
- (30) Bard, A. J.; Salzman, H., *Electroanalytical chemistry*; The Electrochemical Society: 1969.
- (31) Osteryoung, J. G.; Osteryoung, R. A. Square wave voltammetry. *Anal. Chem.* **1985**, *57*, 101–110.
- (32) Ramaley, L.; Krause, M. S. Theory of square wave voltammetry. *Anal. Chem.* **1969**, *41*, 1362–1365.
- (33) Tan, Y.; Wei, X.; Zhang, Y.; Wang, P.; Qiu, B.; Guo, L.; Lin, Z.; Yang, H.-H. Exonuclease-catalyzed target recycling amplification and immobilization-free electrochemical aptasensor. *Anal. Chem.* **2015**, *87*, 11826–11831.
- (34) Bougrini, M.; Baraket, A.; Jamshaid, T.; El Aissari, A.; Bausells, J.; Zabala, M.; El Bari, N.; Bouchikhi, B.; Jaffrezic-Renault, N.; Abdelhamid, E. Development of a novel capacitance electrochemical biosensor based on silicon nitride for ochratoxin A detection. *Sens. Actuators, B* **2016**, *234*, 446–452.
- (35) Mishra, R. K.; Hayat, A.; Catanante, G.; Istamboulie, G.; Marty, J.-L. Sensitive quantitation of ochratoxin A in cocoa beans using differential pulse voltammetry based aptasensor. *Food Chem.* **2016**, *192*, 799–804.
- (36) Badea, M.; Floroian, L.; Restani, P.; Cobzac, S. C. A.; Moga, M. Ochratoxin A detection on antibody-immobilized on BSA-functionalized gold electrodes. *PLoS One* **2016**, *11*, No. e0160021.
- (37) Mejri-Omrani, N.; Miodek, A.; Zribi, B.; Marrakchi, M.; Hamdi, M.; Marty, J.-L.; Korri-Youssoufi, H. Direct detection of OTA by impedimetric aptasensor based on modified polypyrrole-dendrimers. *Anal. Chim. Acta* **2016**, *920*, 37–46.
- (38) Sun, A.-L.; Zhang, Y.-F.; Sun, G.-P.; Wang, X.-N.; Tang, D. Homogeneous electrochemical detection of ochratoxin A in foodstuff using aptamer–graphene oxide nanosheets and DNase I-based target recycling reaction. *Biosens. Bioelectron.* **2017**, *89*, 659–665.
- (39) Abnous, K.; Danesh, N. M.; Alibolandi, M.; Ramezani, M.; Taghdisi, S. M. Amperometric aptasensor for ochratoxin A based on the use of a gold electrode modified with aptamer, complementary DNA, SWCNTs and the redox marker Methylene Blue. *Microchim. Acta* **2017**, *184*, 1151–1159.
- (40) Qing, Y.; Li, X.; Chen, S.; Zhou, X.; Luo, M.; Xu, X.; Li, C.; Qiu, J. Differential pulse voltammetric ochratoxin A assay based on the use of an aptamer and hybridization chain reaction. *Microchim. Acta* **2017**, *184*, 863–870.
- (41) Xiang, Y.; Camarada, M. B.; Wen, Y.; Wu, H.; Chen, J.; Li, M.; Liao, X. Simple voltammetric analyses of ochratoxin A in food samples using highly-stable and anti-fouling black phosphorene nanosensor. *Electrochim. Acta* **2018**, *282*, 490–498.
- (42) Zejli, H.; Goud, K. Y.; Marty, J. L. Label free aptasensor for ochratoxin A detection using polythiophene-3-carboxylic acid. *Talanta* **2018**, *185*, 513–519.
- (43) Zhu, X.; Kou, F.; Xu, H.; Han, Y.; Yang, G.; Huang, X.; Chen, W.; Chi, Y.; Lin, Z. Label-free ochratoxin A electrochemical aptasensor based on target-induced noncovalent assembly of peroxidase-like graphitic carbon nitride nanosheet. *Sens. Actuators, B* **2018**, *270*, 263–269.
- (44) Liu, C.; Guo, Y.; Luo, F.; Rao, P.; Fu, C.; Wang, S. Homogeneous electrochemical method for Ochratoxin A determination based on target triggered aptamer hairpin switch and exonuclease III-assisted recycling amplification. *Food Anal. Met.* **2017**, *10*, 1982–1990.
- (45) Wei, M.; Zhang, W. The determination of ochratoxin A based on the electrochemical aptasensor by carbon aerogels and methylene blue assisted signal amplification. *Chem. Cent. J.* **2018**, *12*, 45.
- (46) Pardee, K.; Green, A. A.; Ferrante, T.; Cameron, D. E.; DaleyKeyser, A.; Yin, P.; Collins, J. J. based synthetic gene networks. *Cell* **2014**, *159*, 940–954.
- (47) Myhrvold, C.; Freije, C. A.; Gootenberg, J. S.; Abudayyeh, O. O.; Metsky, H. C.; Durbin, A. F.; Kellner, M. J.; Tan, A. L.; Paul, L. M.; Parham, L. A. Field-deployable viral diagnostics using CRISPR-Cas13. *Science* **2018**, *360*, 444–448.